

Reduction of Mechanical Stresses in Centrifugal Compressor Impellers for Hydrogen Applications

I. Abd-El-Hussein^a - M. Mäki-Iso^b - J. Tiainen^c - T. Turunen-Saaresti^b - S. Schuster^a - D. Brillert^a

^aChair of Turbomachinery, University of Duisburg-Essen, Duisburg, Germany,
ihab.abd-el-hussein@uni-due.de

^bLaboratory of Fluid Dynamics, LUT University, Lappeenranta, Finland

^cYASKAWA Environmental Energy / The Switch, Lappeenranta, Finland

ABSTRACT

This work focuses on centrifugal compressors utilised in hydrogen pipeline systems and aims to assess the potential to reduce the peak mechanical stress in the impeller by changing the impeller shape. A generic optimisation algorithm is utilised to find an impeller design that significantly reduces the mechanical stress but only slightly penalises the polytropic efficiency. This work starts with a standard impeller design, operated with air. A parameterised model of the impeller is established and is input to an optimisation algorithm. The optimisation algorithm predicts aerodynamic performance with three-dimensional computational fluid dynamics (CFD) and mechanical stress with the finite element method (FEM). By Design of Experiments (DoE) first candidates are generated and analysed. Convergence of the optimisation is monitored and final results are displayed as a Pareto front. The mechanical stress is reduced by a factor of three while the polytropic efficiency drops by three percentage points.

KEYWORDS

hydrogen, compression, mechanical stress

NOMENCLATURE

A Area

h Enthalpy

p Pressure

u_2 Tip Speed

v Specific Volume

ρ Density

η Efficiency

β Angle

δ Thickness

σ_v von-Mises stress

$\sigma_v / \max(\sigma_{v,0})$ Reduced von-Mises stress

0 Properties of baseline compressor

INTRODUCTION

Hydrogen (H_2) is one option to store the energy converted from renewable sources (BMW, 2019; Fuel Cells and Hydrogen 2 Joint Undertaking, 2019). This storage technology can complement other technologies and, in certain cases, can have advantages such as: transport in

existing pipelines and decoupling of storage capacity and power output. Furthermore, H₂ can be used for direct electricity conversion, e.g., in fuel cells (Heinzel, 2009), conversion into mechanical energy (ScienceDirect, 2022), and industrial processes, e.g. in blast furnaces (thyssenkrupp Steel Europe, 2019). Utilising H₂ for the aforementioned applications requires generation, transportation, and conversion into different forms of energy. This paper focuses on onshore transportation; in detail on pressurising and re-pressurising H₂ for transportation in pipelines with centrifugal compressors. While H₂ is generated at pressure levels between 1 - 80 bar (Voitic et al., 2018), the pipeline pressure is in a range between 30 bar to 100 bar (Krieg, 2012). Therefore, an initial pressurisation after generation can be necessary. Pipeline pressure losses have to be compensated by re-compression every few hundred kilometres.

Compared to the transportation of natural gas (CH₄), the main difference from a fluid mechanics and thermodynamics point of view of H₂ transportation is the small molecular weight of H₂ being only one-eighth of CH₄. This corresponds to an increase of the required enthalpy change by a factor of eight for a given pressure ratio (Schuster et al., 2020).

A couple of studies on centrifugal compressors for H₂ transportation suggest increasing the required number of stages for the compression of H₂ in comparison to CH₄ (Tellier, 1981; Heshmat et al., 2010; Bella and Fairman, 2012) or using forward swept blades (Tiainen et al., 2022) while the tip speed is limited to 300 m/s to 600 m/s.

On the other hand, the speed of sound of H₂ increases by the square root of eight. Hence, the compressor can rotate 2.8 times faster while the tip Mach number is the same as for a compressor operated with CH₄. In conclusion, an H₂ and a CH₄ compressor stage can achieve a similar pressure ratio for same tip Mach numbers (Schuster et al., 2020).

The increase of rotational speed is accompanied by an increase of mechanical stresses. Conservative design rules do not allow increasing the tip speed above a threshold value of ≈ 600 m/s. Further research on materials and the reduction of mechanical stresses is required to push this limit to higher values. This paper contributes to the reduction of mechanical stresses by optimising the impeller design.

From a market perspective, the main challenge for applying turbocompressors in recompression stations is the required large number of stages. A larger number of stages means high investment costs for the compressor and the required infrastructure. Increasing the rotational speed allows for reducing the number of compressor stages, but this requires a significant reduction of mechanical stresses. Therefore, the reduction of mechanical stresses is the main objective of this study. On the other hand, aerodynamic performance in terms of efficiency is not the main challenge at the moment. Hence, this study's focus is not on optimising the aero performance.

For retrofitting existing pipeline compression stages, starting with the existing geometry and trying to reduce the mechanical stress can be desirable. A benefit is to reuse several components, manufacture a new impeller, and modify the casing. This approach is pursued in this paper. However, one could also start from sketch and design an entirely new compressor, but this is out of the scope of this paper.

This paper focuses on reducing the mechanical stresses in the compressor impeller while keeping Mach number similarity. The total efficiency of the impeller is considered a measure of the feasibility of the design but is not the main objective of this study. The stage efficiency can be considered later, and many options for optimizing it exists, e.g. diffusor with or without vanes. But these will not reduce the mechanical stress in the impeller directly and presumably not by the required amount. Therefore, this study focuses only on the impeller to reduce the

number of design variables.

From a baseline compressor, a parametric model of the impeller meridional contour and the blade shape is implemented in a computer-aided design (CAD) program. Next, a multi-objective genetic algorithm creates a set of new geometries by varying the CAD model parameters. Aerodynamics performance is evaluated with the help of the 3D-CFD program Ansys CFX, while mechanical stresses are calculated with the FEM program Ansys Mechanical. Results in terms of total-to-total polytropic efficiency and maximum mechanical stress (von-Mises) are passed to the genetic algorithm to develop the next set of geometries. The process continues until no further improvement is detected.

INVESTIGATION METHODS

Baseline Compressor

The closed-loop test stand in the Laboratory of Fluid Dynamics at LUT University, Finland, is used to measure the standard impeller design operated with air. The studied compressor designed at LUT has an unshrouded impeller, nine full and nine splitter blades, a parallel wall vaneless diffuser, a volute and is controlled with active magnetic bearings. The performance measurement setup complies with ISO 5389, and includes the measurements of static pressure and temperature at the compressor stage inlet and outlet; total pressure, total temperature, and static pressure at the impeller outlet; static pressure at the diffuser outlet; ambient pressure and mass flow rate. The steady state of one measurement point is achieved within 15 minutes. Table 1 presents the parameters of the measured compressor.

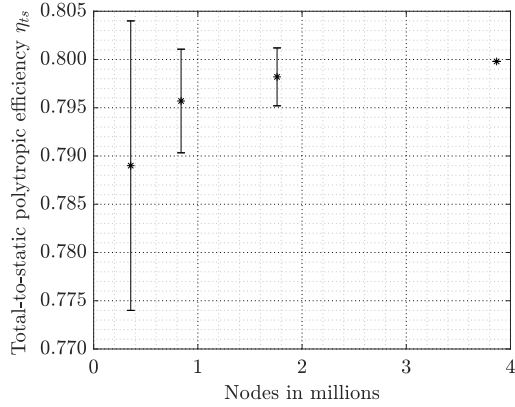
The measurement uncertainties of total-to-static and total pressure ratios are 0.07% and 0.70% due to the higher calibration error of the Kiel probe used for the total pressure measurement at the impeller outlet. The measurement uncertainties of the total-to-static and total-to-total polytropic efficiencies are 0.62% and 0.75%.

Table 1: **Parameters of the baseline centrifugal compressor measured at LUT with air.**

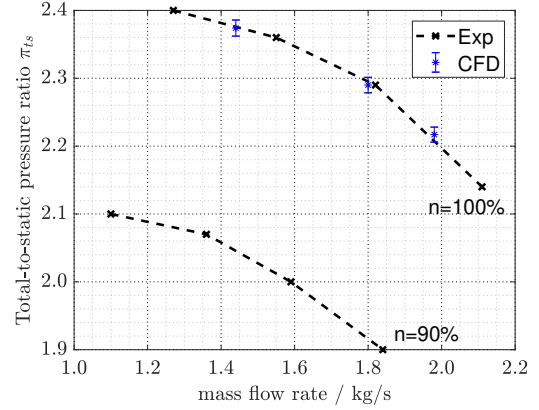
Impeller inlet hub diameter	$d_{1,h}$	40.5 mm
Impeller inlet shroud diameter	$d_{1,s}$	134.9 mm
Impeller outlet diameter	d_2	270.9 mm
Blade height at the impeller outlet	b_2	11.7 mm
Diffuser height	b_3	12.7 mm
Blade backsweep at the impeller outlet	β_2	40°
Tip speed Mach number	$Ma_U = u_2/a_1$	1.15
Relative tip clearance	t/b_2	0.04
Specific speed	$N_s = \omega \sqrt{q_{v1}} / \Delta h_s^{0.75}$	0.70
Rotational speed	n	461 Hz
Mass flow rate	\dot{m}	1.8 kg/s
Total-to-static pressure ratio at the compressor stage outlet	π_{t1-s5}	2.34
Total-to-static polytropic efficiency at the compressor stage outlet	$\eta_{p,t1-s5}$	79.4%

Flow field computation

The blade passage, including one full and one splitter blade, is modelled with periodic boundary conditions. The frozen rotor approach is used at the interfaces between stationary and rotating parts. Total pressure of 20 bar, total temperature of 300 K and 5% turbulence



(a) **Mesh convergence study for the CFD mesh.** Error bars indicate the discretization error.



(b) **Baseline compressor performance map.** Error bars indicate the discretization error.

Figure 1: **CFD Study**

intensity are specified at the inlet of the computational domain. The walls are modelled with adiabatic, no-slip and smooth wall conditions with the turbulence modelled with the SST- $k-\omega$ model. Exit mass flow boundary condition is set at the outlet of the vaneless diffuser. Only a portion of the vaneless diffuser equal to 25 per cent of the impeller diameter is considered during the optimisation. The simulations are performed using steady state solver of Ansys CFX 22.1. Convergence is reached when the domain imbalances are less than 0.1% and the polytropic efficiency is stabilised.

Validation of the CFD results and the mesh independence study are conducted against the experimental data using the full extent of the vaneless diffuser. Computational meshes are realised with the automated meshing software Ansys TurboGrid. The Grid Convergence method (GCI) based on the Richardson extrapolation is used to estimate the discretisation error. Figure 1a depicts the numerical results with the discretisation error for the different meshes. Numerical results show very good matching of the total-to-static polytropic efficiency compared to the experimental result of 0.794 at the design condition. Total-to-static polytropic efficiency is calculated according to Eq. 1 where the kinetic energy at the diffuser outlet is neglected.

$$\eta_{ts} = \frac{\int_{p_{in}}^{p_{out}} v dp - c_{in}^2/2}{\Delta h_t} \quad (1)$$

with v being the specific volume, p being the static pressure, c being the flow velocity and Δh_t being the total enthalpy change. This is done since the static measurements are more reliable at this location. The mesh with around 0.8 million nodes shows around $\pm 0.25\%$ discretisation error, which balances computational load and accuracy.

Comparison of the calculated total-to-static pressure ratio with the performance map of the compressor (1b) also shows a good matching with the selected mesh. The mesh is, therefore, chosen for the remainder of the paper.

Mechanical computation

The mechanical stress is evaluated using the static structural solver of Ansys for a single passage, including one full and one splitter blade. Hub sections of the blades are considered

as fixed support boundaries while imposing a rotational velocity on the domain. Moreover, the effect of the aerodynamic load is considered by importing the pressure distribution over the blades from the CFD results.

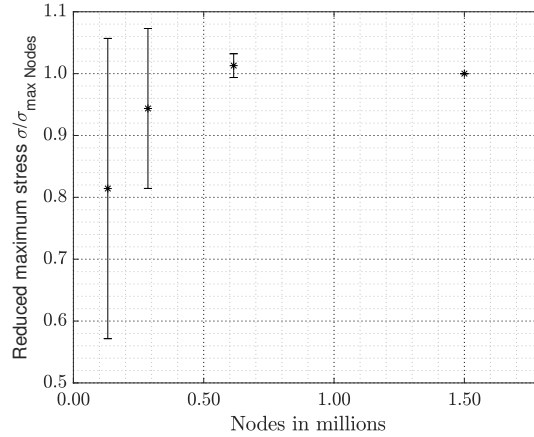


Figure 2: **Mesh convergence study illustrating the calculated maximum von-Mises stress for each mesh divided by the value from the finest mesh. Error bars indicate the discretization error.**

The GCI method is also used for the FEM mesh to obtain a suitable mesh resolution. The maximum von-Mises stress is considered for this study. Figure 2 illustrates the results for four meshes with a grid element refinement factor of 1.3. For the studied geometry, around 0.6 million nodes are sufficient to reach mesh independent results with a discretisation error of 2%. The underlying parameters for this mesh are used in the remainder of this study.

Optimisation algorithm

The optimisation algorithm is based on a multi-objective genetic algorithm that is coupled with the CFD and the mechanical solvers through a CAD model and automated mesh generators. The goal is to optimise the geometry to reduce the peak mechanical stress and to improve the polytropic efficiency. The total-to-total polytropic efficiency is adopted for the optimisation, where the kinetic energy at the outlet of the small diffuser section is considered in the efficiency calculation. This is essential as it represents a large portion of the total energy and because the diffuser optimisation is not in the scope of this paper. The evolution of the results begins from an initial generation created by means of a Design of Experiments (DoE) for the parameterised model of the considered baseline geometry. This is usually done with an initial population of 2^n individuals by considering every combination with the smallest and the largest value of each parameter n . With a total of 14 parameters, this would lead to a very large number of individuals. Therefore, to limit the number of individuals in the initial generation, parameters that are considered to have a highly non-linear effect between the extremities of the optimisation range are implemented randomly, for example, the solid blade angle at the trailing edge. The geometry is optimised regarding the meridional contour and the blade shape. The meridional contour is modelled with Bezier curves to ensure a smooth geometry. Figure 3 depicts the selected control points for the optimisation with the corresponding degree of freedom.

Impeller blades are optimised on two layers, at the hub and the shroud, by considering

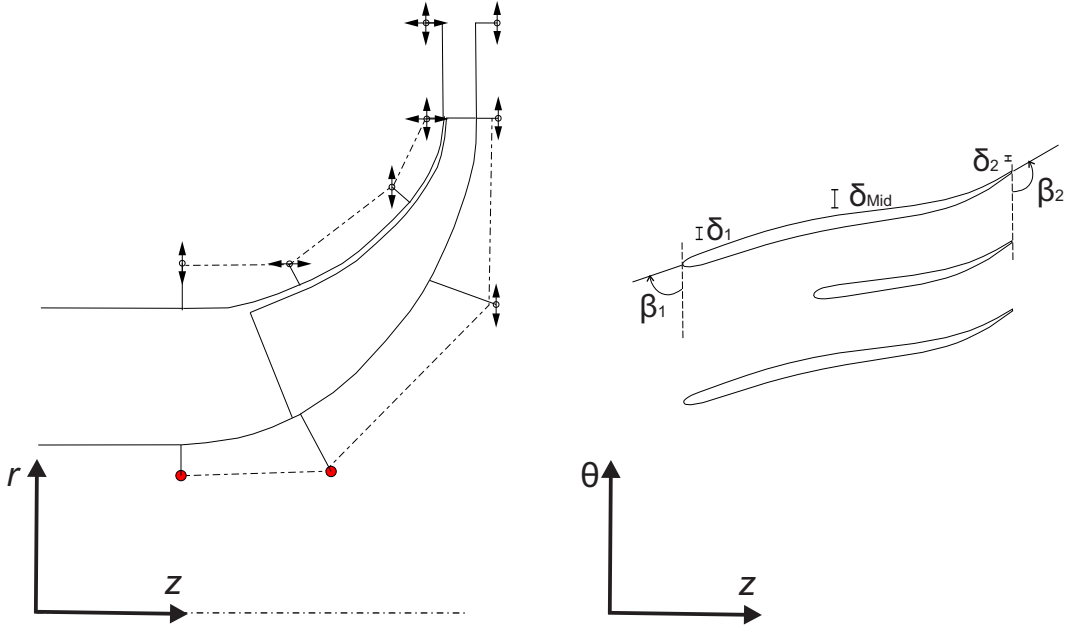


Figure 3: **Parameterised model for the meridional contour and the blade shape of the baseline geometry.**

prismatic blading. Eight parameters are considered for the blades optimisation, including the blade angles β at the trailing and the leading edges, the meridional location of the main and the splitter blade and the thickness δ distribution. The latter is imposed at the hub layer following a Gaussian distribution while a linear variation is implemented at the shroud.

Results

Baseline Compressor

Starting from the values for the compressor operated with air, Mach number similarity analysis is used to obtain the rotational speed and mass flow rate for the compressor operated with H_2 according to Eq. 2 and Eq. 3, respectively.

$$u_{2,air}/a_{air} = u_{2,H_2}/a_{H_2} \quad (2)$$

$$\dot{m}_{air}/(a_{air} \cdot \rho_{air} \cdot A_0) = \dot{m}_{H_2}/(a_{H_2} \cdot \rho_{H_2} \cdot A_0) \quad (3)$$

with u_2 being the solid blade peripheral velocity at the trailing edge, a being the speed of sound at the inlet and ρ being the inlet density. As H_2 and air have nearly equal specific heat ratios, holding the rotational Mach number similarity (Eq. 2) leads to comparable values of the pressure ratio. With the latter being normally a design constraint. This results at the selected hydrogen inlet boundary conditions of 20 bar and 300 K in a rotational speed of around 106000 rpm.

During the optimisation, the blade angle at the trailing is allowed to vary from the baseline value of -40° (back swept) up to 20° (forward swept). The effect of this high variation on the work coefficient is considered by reducing the rotational speed linearly by a maximum amount of 8% for the highest forward swept blade. On the other hand, imposing a constant axial Mach number (Eq. 3) permits to match the inlet velocity to the much increased blade

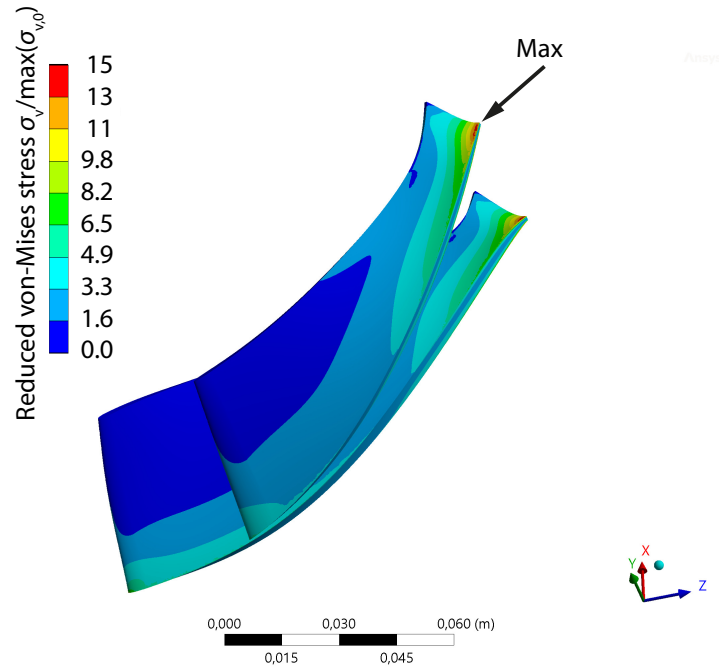


Figure 4: **Contour plot of reduced von-Mises stress for the baseline geometry operated with H_2 .**

peripheral velocity. This is done at the consequence of a variable mass flow rate that changes with the inlet area.

For the remainder of the paper, the reduced von-Mises stress $\sigma_v / \max(\sigma_{v,0})$ is plotted, which is calculated by dividing the von-Mises stress by the maximum von-Mises stress occurring for the baseline compressor operated with air at design rotational speed. Figure 4 illustrates the reduced von-Mises stress of the baseline geometry with H_2 . As expected, the high rotational speed causes an enormous increase in the mechanical stress that reaches up to a factor of 15 for the studied geometry. On the contrary, by respecting the Mach number similarity while neglecting the geometry deformation, an increase of around 2 percentage points in the polytropic efficiency is found. This increase can be related to the nearly one order higher Reynolds number when operating the compressor with H_2 .

Pareto Front

From the initial population, the solution evolves towards a global Pareto-front. That is the set of geometry that describes the best value that can be reached for an objective while the other objective is fixed.

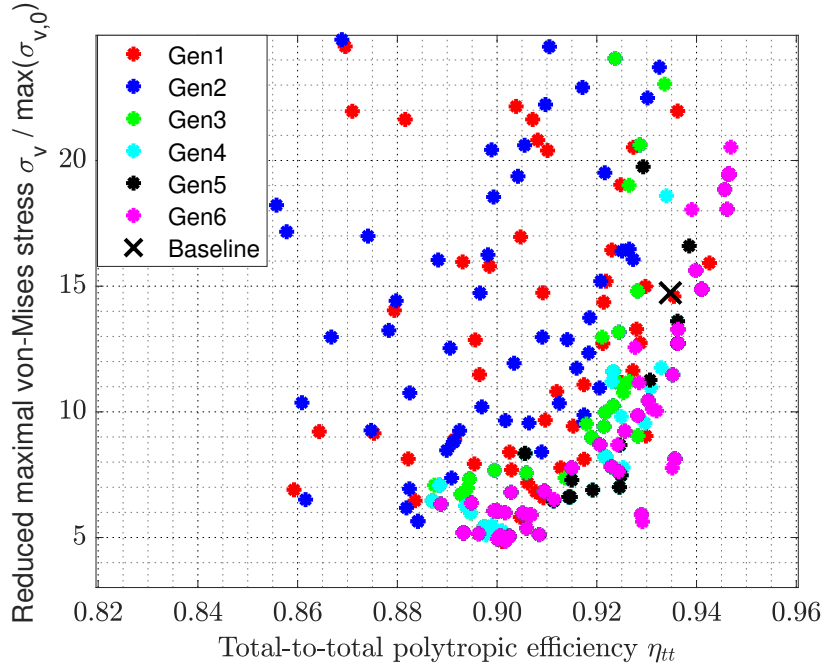


Figure 5: **Results of the different generations that evolved during the optimisation each with a different color.**

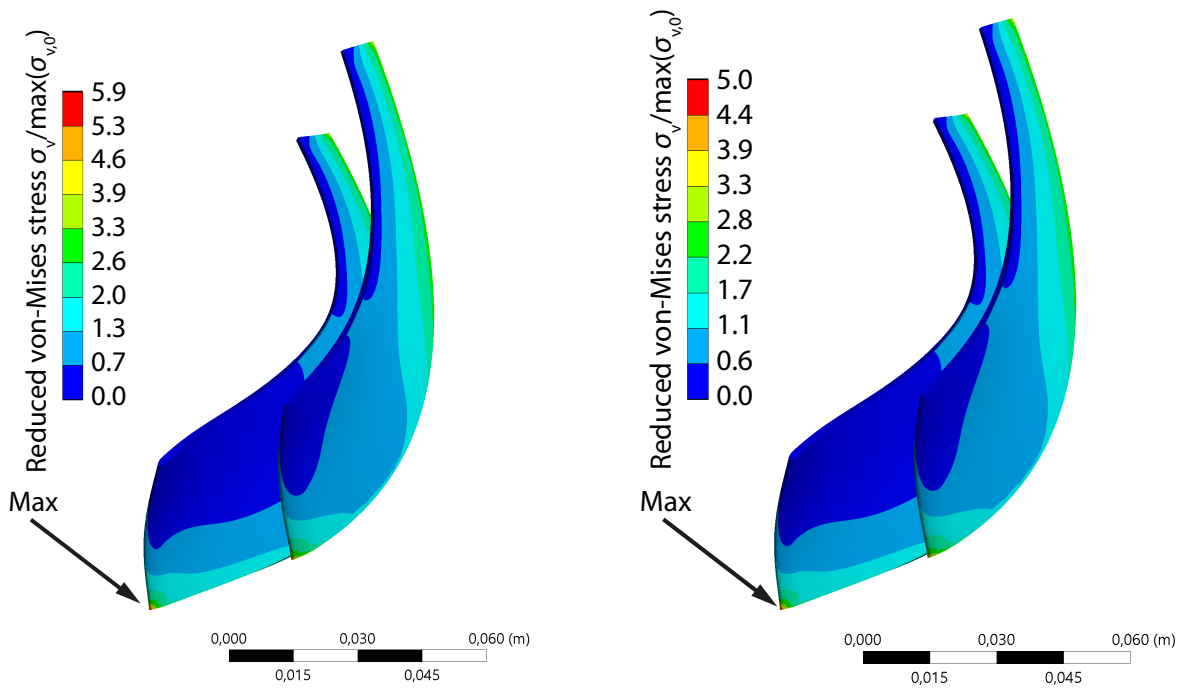
Figure 5 shows the results of the optimisation for the different generations in terms of the optimised parameters, while the black cross represents the baseline performance. Reduction of the reduced maximal von-Mises stress from around 15 for the baseline geometry down to around 5 is achievable at the expense of losing about 3 percentage points in efficiency. Yet, a reduced maximal von-Mises stress of 6 is reached with a penalty of less than one percentage point in efficiency.

The impact of the different parameters is considered against the objectives to extract guidance for the design of hydrogen compressors. While most parameters showed a scattered effect on the results, two parameters showed a distinct correlation. These are the blade trailing angle and the outer radius of the impeller. The reason for that can be directly related to the reduction in the rotational speed. While the peripheral velocity at the trailing edge is held constant, increasing the outer radius leads to lower rotational speed. Similarly, the rotational speed is lowered when going from backward swept blades to forward swept blades to hold a constant work coefficient. However, both of these parameters have a negative impact on the efficiency. Limiting the blade forward sweeping angle to 5 degrees provides an acceptable trade-off between efficiency and mechanical stress.

Selected Geometry

To further investigate the results of the optimisation, one of the best performing geometries from the Pareto-front is selected for detailed inspection. The selected geometry has a total-to-total efficiency of 0.927 and a reduced maximal von-Mises stress of 5.9. Compared to the baseline geometry, the optimised one features an extended outer diameter, main blades that are fully extended to the inlet of the impeller, a slightly backwards swept blade and a chamfer at

the trailing edge towards the hub layer.



(a) Optimised geometry with a total-to-total efficiency of 0.927.

(b) Optimised geometry with lowered rotational speed of 90000 rpm.

Figure 6: Reduced von-Mises stress

This results in a reduction of the maximal mechanical stress as depicted in Fig. 6a. Moreover, the location of the maximum stress is moved from the trailing edge to the hub layer at the leading edge. At this location, reducing the maximum stress by increasing thickness is expected to have a much lower impact on the aerodynamic performance than modifying the trailing edge geometry. Distinct aerodynamic features that have a clearly positive effect on mechanical stresses cannot be identified. It turns out that aerodynamic features are scattered throughout the design space.

Geometry optimisation is only constrained by the Mach number similarity. However, due to the high variation of the impeller shape, numerical results of the total pressure ratio showed a high variation from around 2.4 to 3.1. For instance, the selected geometry has a total pressure ratio of 2.97, which is much higher than the total pressure ratio of the baseline geometry being 2.55. This allows for a reduction of the rotational speed and, therefore, for a further reduction of the mechanical stress. Decreasing the rotational speed by 8% to reach 90000 rpm leads to the design total pressure ratio of 2.55. Figure 6b illustrates the reduction of the maximum von-Mises stress under this condition where an additional improvement of around 15% from 5.9 to 5 is achieved.

Conclusion

This paper considers the optimisation of the impeller of centrifugal compressors utilised for pipeline compression. When applying the Mach similarity on a baseline compressor, numerical results show that the maximum mechanical stress increases to around 15 times that at the design

speed when operated with air leading to a stress level that exceeds material limits. By combining a genetic algorithm with a CFD and a structural mechanics solver, reduction of the maximum stress to the third is achieved while the efficiency is only penalised by less than 3 percentage points.

Results of the optimisation show that the maximum stress is still beyond the limits of most materials. Therefore, a slight decrease in the circumferential Mach number or the addition of other parameters for further optimisation might be required. Moreover, results show that the impeller outer radius and the blade angle at the trailing edge directly correlate with the mechanical stress. Where increasing the former and going in the direction of forward swept blade angle for the latter reduces the stress. However, both parameters show a negative effect on the total-to-total efficiency. Particularly for the blade angle, results suggest that it should be limited to around 5 degrees in order to have a balanced effect between the reduction of the mechanical stress and the deterioration of the total-to-total efficiency.

REFERENCES

- Francis A. Di Bella and Kevin D. Fairman. Development of a 240,000 kg/day hydrogen pipeline centrifugal compressor for the department of energy's hydrogen delivery and production program. In *Proceedings of the ASME 2012 International Mechanical Engineering Congress and Exposition*. American Society of Mechanical Engineers, 2012. doi: 10.1115/imece2012-88965.
- BMW. Wasserstoff und Energiewende, 2019. URL <https://www.bmwi.de/Redaktion/DE/Downloads/J-L/kurzpapier-wasserstoff.pdf>. Accessed: 29.01.2020.
- Fuel Cells and Hydrogen 2 Joint Undertaking. *Hydrogen roadmap Europe : a sustainable pathway for the European energy transition*. Publications Office, 2019. doi: 10.2843/341510.
- Angelika Heinzl. *Fuel cells and hydrogen technology*, pages 368–373. Springer Berlin Heidelberg, Berlin, Heidelberg, 2009. ISBN 978-3-540-88546-7. doi: 10.1007/978-3-540-88546-7_69.
- Hooshang Heshmat, Andrew Hunsberger, Zhaohui Ren, Said Jahanmir, and James Walton. On the design of a multi-megawatt oil-free centrifugal compressor for hydrogen gas transportation and delivery: Operation beyond supercritical speeds. In *Proceedings of the ASME 2010 International Mechanical Engineering Congress and Exposition*, 2010. doi: 10.1115/imece2010-40575.
- Dennis Krieg. *Konzept und Kosten eines Pipelinesystems zur Versorgung des deutschen Straßenverkehrs mit Wasserstoff*. Schriften des Forschungszentrums JÄ¼lich, Reihe Energie und Umwelt, Energy und Environment, Band 144, 2012. ISBN 978-3-89336-800-6.
- Sebastian Schuster, Hans Josef Dohmen, and Dieter Brillert. Challenges of compressing hydrogen for pipeline transportation with centrifugal-compressors. In *Proceedings of Global Power & Propulsion Society*. GPPS, September 2020.
- ScienceDirect. Hydrogen engine, 2022. URL <https://www.sciencedirect.com/topics/engineering/hydrogen-engine>. Accessed: 20.10.2022.

C Tellier. Application of axial flow compressors for long distance pipeline transmission of hydrogen. *International Journal of Hydrogen Energy*, 6(4):413–422, 1981. doi: 10.1016/0360-3199(81)90066-5.

thyssenkrupp Steel Europe. World first in Duisburg as NRW economics minister Pinkwart launches tests at thyssenkrupp into blast furnace use of hydrogen, 2019. URL <https://www.thyssenkrupp-steel.com/en/company/sustainability/climate-strategy/>. Accessed: 29.01.2020.

Jonna Tiainen, Sebastian Schuster, T. Turunen-Saaresti, M. Mäki-Iso, and Dieter Brillert. "hydrogen compression - towards a new strategy for the design of hydrogen compressors. In *Proceedings of ASME Turbo Expo 2022*. "ASME, June 2022.

Gernot Voitic, Birgit Pichler, Angelo Basile, Adolfo Iulianelli, Karin Malli, Sebastian Bock, and Viktor Hacker. Hydrogen production. In *Fuel Cells and Hydrogen*, pages 215–241. Elsevier, 2018. doi: 10.1016/b978-0-12-811459-9.00010-4.